Proceedings of Nuclear and Emerging Technologies for Space 2009
Atlanta, GA, June 14-19, 2009
SAND2009-1202C

METHODS FOR MODELING IMPACT-INDUCED REACTIVITY CHANGES IN SPACE REACTORS

T. R. Radel, R. F. Radel, J. A. Smith and R. J. Lipinski
Sandia National Laboratories
P.O. Box 5800, Albuquerque, NM 87185
Tel: 505-844-7937, Fax: 505-844-2829, Email: tradel@sandia.gov

P. H. H. Wilson
University of Wisconsin
Madison, WI
Tel: 608-263-0807, Fax: 608-263-0807, Email: wilsonp@engr.wisc.edu

Abstract – *This paper describes techniques for determining impact deformation and the subsequent reactivity change for a space reactor impacting the ground following a potential launch accident. This technique could be used to determine the margin of subcriticality for such potential accidents. Specifically, the approach couples a finite element continuum mechanics model (PRONTO3D or PRESTO) with a neutronics code (MCNP). DAGMC, developed at the University of Wisconsin-Madison, is used to convert PRONTO3D output to a usable MCNP input file. This paper summarizes what has been done historically for reactor launch analysis, describes the impact criticality analysis methodology, and presents preliminary results using representative reactor designs.*

I. INTRODUCTION

In the past, significant research has gone into space reactor designs for various programs. Calculations have been performed to demonstrate criticality safety both on Earth and while in orbit. Since the radiological inventory of a nuclear reactor is very small prior to initial operation, it is very desirable to design the reactor so that it does not become critical during a launch accident. Past analyses have primarily involved criticality calculations for reactors immersed in water, wet sand or other materials, but without distortion of the initial geometry. This paper describes a method for assessing the effects of reactor distortions resulting from ground impact.

II. PREVIOUS WORK

The only launch of a nuclear reactor into space by the U.S. was SNAP-10A, which was launched on April 3, 1965.[1] Four hours after launch, reactor startup was initiated and full power (600 kWe) was achieved nine hours after startup. It operated smoothly for 43 days until a spacecraft electronic fault caused an automatic and permanent shutdown. Since then there have been numerous concepts for space reactors developed to various levels of detail by the U.S., but none have been built or launched into space.

The SP-100 program developed a fairly detailed concept for a 100 kilowatt electric (kWe) reactor power system based on a lithium-cooled uranium nitride (UN) fueled fast reactor and SiGe thermoelectric power conversion.[2] The program also developed and tested some key hardware, including the UN fuel pellets, control drive motors, and prototype heat exchangers. The program was canceled before a reactor could be constructed.

The Jupiter Icy Moons Orbiter (JIMO) program and the subsequent Prometheus program developed several top-level concepts for multi-hundred kWe reactor power systems.[3] The dominant options for the reactor were lithium cooled, heatpipe cooled and He/Xe cooled. Sodium, NaK, and water cooled systems were also considered. Power conversion options included thermoelectric, Stirling and Brayton conversion. The level of detail achieved for these concepts was not as great as for the SP-100 program when the Prometheus program was canceled.

More recently NASA has been considering fission surface power systems for a lunar base.[4,5] NaK cooled reactor concepts with Stirling power conversion have been reported. Prior to this, NASA and others had considered small reactors for Mars and other missions.[6,7]

In addition to the nuclear electric power systems described above, the U.S. has developed concepts and hardware for nuclear thermal propulsion systems. The Rover/NERVA project produced fairly detailed designs and operating hardware that concluded with several ground tests of a thrusting reactor/rocket that heated hydrogen in the reactor core to develop thrust.[8,9] The program culminated with the Pewee reactor thrusting for a total of 40 minutes at full power, including two restarts. Calculations were performed to assess the criticality increase from a postulated reactor impact during a launch accident. An experiment with a reactor was performed with a reactivity increase rate comparable to the projected rate from a strong impact to help estimate the energy release in such an event[8,9]

The Space Nuclear Thermal Propulsion (SNTP) program developed nuclear thermal reactor concepts using particle fuel.[10] It produced a fairly high-fidelity criticality experiment and culminated with element testing driven by an external reactor. Neither the Rover/NERVA program nor the SNTP program resulted in launch of a reactor.

For all the programs described above, safety of the system during launch and subsequent operation was always a key consideration in the design process. Particular attention was given to accidents that might occur during the launch process. All of the concepts used highly enriched uranium and it was recognized that prior to operation the radiological inventory of the reactor is very low (typically less than 10 Ci (3.7×10^{11} Bq)). Such a low level of activity would have extremely low health and environmental consequences if there were a launch accident that dispersed the reactor material.

To take advantage of the very low levels of radioactivity in a fresh space reactor, a common approach to safety in these past programs was to avoid operation of the reactor prior to launch and achieving a stable deployment (e.g. on the Moon), trajectory, or orbit. In addition, the reactor would be launched in a substantially subcritical state. Finally, the reactor designs considered environments that might increase the reactivity during a launch accident and materials and geometries were developed to minimize or overcome these potential reactivity increases.

The most commonly addressed source of potential reactivity increase was the submersion of the reactor in water or wet sand near the launch pad. Space reactor concepts use highly enriched uranium to reduce the total system mass needed to achieve criticality, but this leads to the potential that water could moderate the neutrons and increase reactivity. One solution to this issue is a spectral-shifting neutron absorber.[11,12] A spectral-shifting absorber (e.g. Gd or Eu) does not absorb fast neutrons very effectively, but does absorb thermal neutrons fairly readily. This counters the increase in fission cross section as the neutrons are thermalized by water. Another solution is the use of an external neutron reflector that is better at reflection than water (e.g. BeO). Replacement of the reflector by water results in a net decrease in reflection and compensates for the increase in fission cross section.

In most of the past analyses the effect of the water, wet sand, and other accident environments was assessed without formally addressing the potential for deformations due to the accident. Part of the reason for this may have been the difficulty in performing impact calculations. However, the development of finite element continuum mechanics codes and parallel processing computers has reached the point where such calculations are becoming feasible. This paper presents a methodology for performing impact calculations, and mapping the results into a neutron criticality code. It also presents some preliminary results for representative reactor configurations to give some insights on the margins that might be available against impact criticality.

III. BOUNDARY CONDITIONS

Potential launch accident scenarios that might lead to distortion of the reactor geometry include blast and impact. Blast effects from liquid propellant are typically much lower than the effects of impact onto the ground.

The amount of potential distortion to a reactor during impact is a function of the reactor and surrounding geometry, the impact velocity, and the impacted surface. For purposes of development of the methodology, a representative set of conditions was chosen for the impact and the reactivity calculations.

Typical surfaces that a spacecraft or reactor might impact during a launch accident are concrete, steel, asphalt and sand. The impact velocity depends on the spacecraft or reactor height at the time of the accident, the mass of the system, its cross-sectional area and its drag coefficient. Table I gives the impact velocity for a drop from various heights neglecting air resistance. For reference, the height of a payload on the proposed Ares V launch vehicle is about 100 m, so the impact velocity for a launch with this vehicle is likely to be greater than 44 m/s. The terminal velocity for a fully fueled lunar lander (about 45,000 kg with a diameter of 8 m) is about 120 m/s. The terminal velocity for the reactor power system described by Marcille[4] (2200 kg with water shield, no attached radiator and a diameter of 1 m) is about 210 m/s if falling core first. However, it takes a large initial height to achieve 210 m/s, and the launch vehicle could be over sand by that time. The maximum impact velocity on concrete at the launch pad is about 100 m/s. A lower bound velocity of 40 m/s will be used for the calculations in this scoping study.

TABLE I

Impact Velocity Neglecting Air Resistance

Height (m)	Velocity (m/s)
100	44

200	63
400	89
1000	140
2000	198

The material surrounding the reactor following impact is a function of the initial configuration and other environmental factors. Usually water or wet sand is assumed so as to give the greatest effect on enhancing reactivity (to yield a conservative calculation). It may be difficult to envision a reactor ending in water following impact on concrete. But there may be the potential to bounce into a nearby flame pit or depression where water spray from the acoustic suppression system might have accumulated. So water will be assumed as one possible medium that could surround the reactor. For scoping purposes, other potential materials for consideration are wet sand and liquid hydrogen (undergoing film boiling on the surfaces of the reactor vessel).

IV. COUPLING METHODOLOGY

To assess the reactivity increase from impact, first a continuum mechanics code is used to determine the amount of distortion. Once the continuum-mechanics simulation of the impact is complete, the resulting deformed geometry needs to be imported into a neutronics code to determine the resulting reactivity (ρ) or neutron multiplication (k_{eff}). The neutronics code selected for this task is MCNP. Several applications have been developed for importing CAD-generated geometries into MCNP[13]. But importing a distorted geometry following impact is much more challenging. The resulting geometry can no longer be described by a small set of simple shapes. Nonetheless, a CAD-to-MCNP code can be used as a basis for developing the post-impact import capability.

The code selected for this development couples the Direct Accelerated Geometry Monte Carlo (DAGMC) software library[14] being developed at the University of Wisconsin, with MCNP5 (hereafter referred to as DAG-MCNP5). DAGMC is based on the Mesh Oriented dAtaBase (MOAB)[15] project of the Interoperable Tools for Advanced Petascale Computing (ITAPS) program, and includes methods to perform efficient ray-tracing on mesh-based representations of solid model geometries. When combined with the Common Geometry Module (CGM), CAD-generated solid models are converted to mesh-representations using the facets that are generated by the solid modeling engine itself. For this project, the mesh is generated for the purpose of the impact calculation, and that mesh is used for the radiation transport. The workflow of this analysis needs to be carefully considered and leads to some new developments in DAGMC required to support this coupling.

IV.A. Analysis Workflow

The mesh-generation for the impact calculation component of this analysis is performed using the CUBIT[16] tool, the output of which is a file that contains both geometry and mesh information, and the relationship between the two. The ability to associate mesh with geometry in DAGMC allows for more efficient ray-tracing on the surface elements of the mesh. CUBIT can also export a mesh-only file in the Exodus II format used by PRONTO3D/PRESTO[17,18] continuum mechanics codes for both input and output. DAGMC reads first the pre-deformation CUBIT mesh/geometry data to define the ray-tracing geometry, and then reads the post-deformation Exodus II formatted output of the impact simulation to update the location of the nodes in the mesh. This geometry is then used to perform Monte Carlo radiation transport/criticality calculations using DAG-MCNP5.

IV.B. DAGMC Developments

Most of the capabilities necessary to support this workflow are already part of the MOAB capabilities, or are capabilities that may be broadly applicable to MOAB users beyond this project. The ability to read the CUBIT geometry/mesh files and Exodus II mesh files was already built-in to MOAB, but using one to update the node locations of the other is a new feature that has been added. Because the mesh used for impact simulation is a hexahedral mesh and DAGMC requires triangular surface elements for efficient ray-tracing, a method to convert quadrilateral elements to triangular elements has been implemented. These simple additions are sufficient to support the workflow for simple geometries, but more advanced developments are needed for real reactor geometries.

Typical solid model representations of real systems do not include an explicit representation of non-solid parts of the system, known as the *complement*. In the case of the reactor geometries to be modeled in this project, these include coolant regions, vacuum regions and gas plenum regions. While DAGMC is able to automatically recognize these regions, it is not able to distinguish among them. Rather, they are modeled as a single complex disjointed region, to which one set of material properties may be assigned for the radiation transport calculations. For well-defined geometries such as this, however, an algorithm is under development to identify closed bounding surfaces and their topological relationship so that separate regions can be defined, each with their own material properties.

Due to the associated computational cost savings, one common approach in continuum mechanics simulation is to model thin layers as so-called *shell elements* that have no volume, but do have the mass and stiffness of material in question. In this project, fuel pin cladding will be modeled using shell elements to accelerate the impact simulations. However, since the Monte Carlo radiation transport process expects all materials to have volume,

special treatment of these shell elements will be required. While one approach is to simply ignore them and account for those materials by homogenizing them with other materials, there could be places where these shell elements are the only thing dividing two regions of the complement (e.g. cladding separating the coolant and fission gas plenum), so this will need to be accommodated.

Finally, a potential outcome of the impact is the failure of independent mesh elements representing tearing and/or fracture. This is most likely to occur on material boundaries and therefore represents a change in the geometric topology. The mesh update process will need to be able to recognize these *dead elements* and properly modify the relationship between geometry/materials and mesh. New methods are being designed to perform this operation and estimate its impact on the accuracy of the criticality calculation.

IV.C. Initial Test Cases

A simple cylinder was used for the initial test of the coupling capability between the impact analysis code and DAG-MCNP5. This single volume was used to demonstrate the work flow before more complicated features are added to the geometry, s*hell elements* or *dead elements* for example. The details of this analysis will be discussed in the following sections.

A second test was performed to compare the results of a hand-made MCNP deck with the results from a DAG-MCNP5 deck. A significantly more complicated, 19-pin rector, geometry was used for the study. The reactor was modeled in both MCNP and SolidWorks. The SolidWorks model was then imported into Cubit for geometry manipulation. Overlapping and duplicate surfaces were resolved and it was then exported as an ACIS geometry file for input into DAG-MCNP5. The geometry and results from this design will be discussed in further detail in Section VI.

As a comparison for future reactor impact analyses, the 19-pin reactor model was altered by hand to an approximated post-impact geometry. A qualitative assessment of actual impact results from Pronto3D[17] was used as a basis for the geometry deformations. Reactivity in various surrounding mediums was looked at.

V. IMPACT ANALYSIS RESULTS

The finite element analysis (FEA) work flow consists of developing the geometric model using CUBIT[16], conducting the computation using the explicit Lagrangian finite element (FE) code for modeling transient solid mechanics problems, Pronto3D[17], and outputting the deformed shape as a function of time in the Exodus[18] format. To test the workflow and compatibility of the communication between the structural analysis code and the neutron criticality code a simple geometry was created and an impact analysis performed. The structural analysis results were passed to the criticality code to flush out any initial compatibility issues.

The simple geometry for this test problem is a right circular cylinder (height=38 cm, diameter=24 cm) of UO_2-like material that is impacted into a pad of steel with properties of A36 steel[19] at 40 m/s. Figure V.1 presents the undeformed meshed geometry and the resulting deformed geometry.

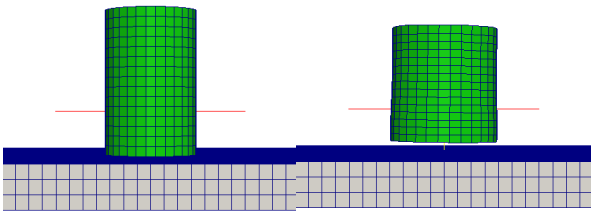

a) undeformed b) deformed

Figure V.1. Initial test geometry.

Currently, the characterization of the mechanical material properties of UO_2 material for impacts at the velocities in the range considered here is not well characterized. An initial literature search did not yield any such properties. Therefore, for the analyses presented here the "Soil-n-Foams" constitutive model[17] implemented in Pronto3D was applied using what the authors consider to be UO_2-like properties. The Soil-n-Foams model uses a pressure-dependent yield surface to describe the relationship between the pressure and volumetric strain.

The next analysis performed was a 40 m/s impact of the inner core portion of the 19-pin reactor presented in Section VI.B below. For the structural impact simulation the structure impacts a pad with the properties of A36 steel. The structural model consisted of the vessel that contains the 19 pins, inner basket which holds the fuel pins, and the fuel pins (containing fuel and reflector pellets). No other materials were modeled. All components were modeled using 8-node hexagonal (hex) elements except for the fuel cladding which was modeled using 4-node shell elements.

The fuel in each fuel rod was modeled as a continuous cylinder of fuel (i.e., individual pellets were not modeled). Again, the UO_2 properties were approximated with the Soil-n-Foams model. The outside diameter (O.D.) of the cylinder of fuel and the reflector pellets matched the O.D. of the fuel pins. The clad shell thickness was specified as the same as that noted in Table III, but the centerline of these shells are located at the O.D. of the fuel rods. The fuel pins were modeled in this way to ensure that the geometry passed to the criticality code was consistent with the geometry of the undeformed structure. The criticality

code is not currently capable of taking into account the volume of components modeled with shell elements. Therefore, the fuel and reflector pellets had to include the thickness of the cladding.

The vessel, fuel basket, fuel caps, and cladding were all modeled using an elastic-plastic power law hardening material model with properties compatible with 316 stainless steel[20]. As with the simple problem discussed above, the impacted pad had A36 steel properties and the fuel used UO_2-like materials. At the time of the analysis the mechanical properties for the reflector pellets were not characterized. To distinguish them from the fuel material they were modeled with the same A36 properties as the impacted pad.

The analysis did not implement any method to include tearing, fracture, or any other form of breaking of material. The 19 fuel pins were free to move and interact with surrounding fuel pins and the basket. The basket and the fuel pins were free to move inside of the vessel. The simulation impact time was for 0.100 seconds. This is enough time for the structure to impact and rebound off the impacted pad. The final deformed shape was transferred to the criticality code.

A view of the model before impact is shown in Figure V.2. The figure shows the portion of the 19-pin reactor modeled with part of the vessel, fuel basket, and some of the fuel pin cladding removed to show the interior of the structure modeled and how the fuel and reflector pellets are included in the model. The vessel is shown in steel-blue color, the basket shown in yellow, and the fuel rod cladding and caps shown in green, reflector pellets in red, and the fuel in blue.

Figure V.3 is presented to show the relative mesh refinement for the pad, vessel, fuel basket, and fuel pin cladding. For expediency of the calculation the exterior vessel of this model was meshed with a relatively coarse mesh. The fuel basket used a finer mesh. The finest mesh was reserved for the fuel pins (including the reflector pellets and fuel). The mesh refinement of the reflector pellets and fuel was uniform throughout their length. The model has a total of approximately 3.6 million elements and 4.0 million nodes.

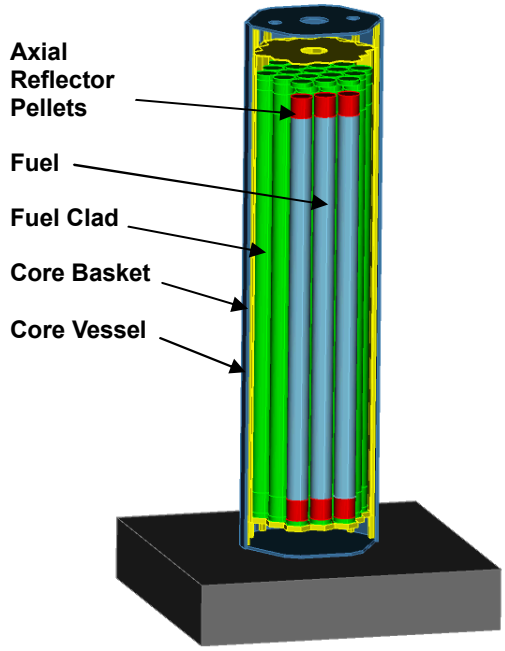

Figure V.2. Geometry of 19-pin reactor FEA model.

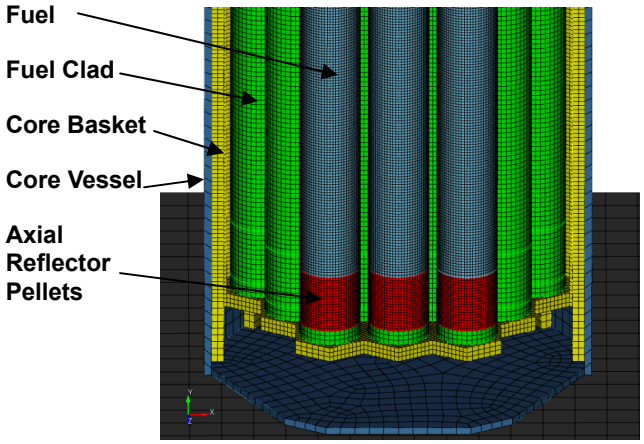

Figure V.3. Meshed detail of 19-pin reactor FEA model

The analysis was performed using the Capacity Computing and Visualization clusters at Sandia National Laboratories. The 19-pin geometry analysis was performed using 300 processors and ran for approximately 24 hours. The overall deformed shape of the geometry (with a portion of the vessel and fuel basket removed for visualization purposes) is shown in Figure V.4. The rippled surface on the fuel pins is the steel clad. The fuel pins have become shorter in length and larger in diameter from the impact. Again, this is a preliminary result which may change in detail as the characterization of the mechanical material properties of UO_2 is improved. Figure V.5 is presented to show the resulting deformed shape of the fuel which has been used as the basis for the MCNP results presented in the next section.

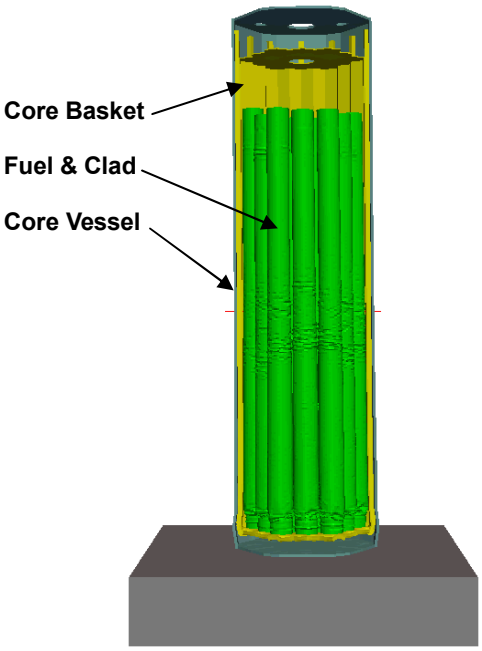

Figure V.4. Resulting deformed geometry of portion of 19-pin reactor modeled in the FEA.

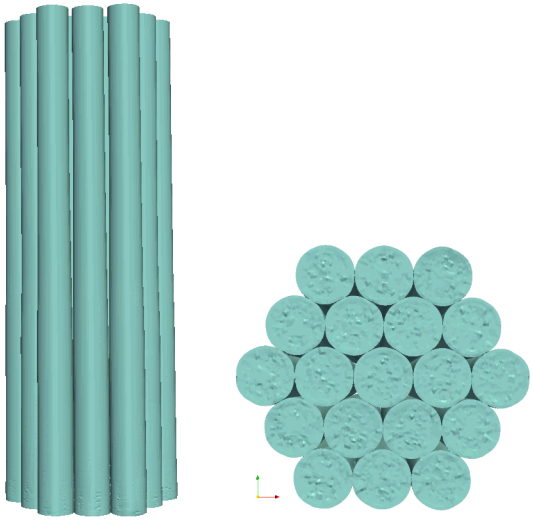

a) Side view b) Bottom view

Figure V.5. Resulting deformed shape of fuel in the 19-pin reactor.

The 19-pin model analysis results demonstrate some of the capabilities of current technology. However, there are a number of technical issues that remain to be addressed to enable the application of this methodology to an actual accident scenario. The analysis presented here includes only a portion of the overall reactor. The complete reactor structure is a much more complicated structure with a variety of materials that need to be characterized for loading rates in the dynamic regime of potential accidents. In addition, some of the potential materials are not solids (e.g. the reactor coolant) and therefore their behavior is difficult to account for in a traditional finite element code. Some of these issues have implications with respect to the compatibility between the FEA and the criticality analysis. For example, the best method to implement shell elements and potential issues that arise from the implementation of FEA techniques such as element death as an approach to model material failure are challenges that still lay ahead. It is the intent of the authors to address some of these issues in future work.

VI. MCNP RESULTS

VI.A. Results from Impact/Neutronics Coupling

The workflow of the coupled impact simulation and criticality calculation was tested with a simplified problem consisting of a single right circular cylinder (R=12 cm, H=38 cm) of 93% enriched UO_2 (ρ=10 g/cm^3) in a vacuum. A coarse mesh was applied to this geometry (1215 elements in the cylinder).

Table II shows a summary of results from a simulation using the native geometry format of MCNP5, the solid model-based faceted geometry representation of DAG-MCNP5 (with different faceting approximations), and the mesh-based geometry representation of DAG-MCNP5 for use in this workflow. All cases had 5000 histories per generation with 25 inactive and 100 active cycles. Most apparent in the results is the volume discrepancy among the various geometry representations. It is clear that the different faceting/meshing tolerance results in underestimation of the total volume of fissile material which has an impact on the calculated value of k_{eff}. It will be important to ensure that the meshing is fine enough to provide a good approximation of the volume of each region. The 0.73% missing volume results in a 0.31% underestimation of k_{eff}, a difference of nearly 4σ.

TABLE II. Results of test problem using different MCNP5 geometry representations

Geometry Representation (Faceting tolerance)	Cylinder Volume [cm3]	Surface Facets (cylinder)	k_{eff} (std dev)
Native	17190.8	9 (3)	0.98373 (0.00080)
Solid Model (10^{-3})	17188.9	1028 (972)	0.98179 (0.00085)
Solid Model (10^{-4})	17190.6	3132 (3076)	0.98363 (0.00100)
Solid Model (10^{-5})	17190.8	9788 (9732)	0.98391 (0.00099)
Mesh	17065.4	9312 (612)	0.98077 (0.00089)

VI.B. 19-pin Rector Studies

The simple 19-pin reactor was used to test the accuracy of the DAGMC conversion process with respect to neutronics. The geometry was also modified to an approximated post-impact configuration. Calculations were performed on all three files (standard MCNP, DAGMC, and approximated post-impact MCNP) with multiple surrounding materials.

As the approach discussed in this paper will ultimately be tested on an 85-pin reactor concept[4], a simplified 19-pin version of this reactor was developed for some initial model testing. Various design parameters are listed in Table III and the configuration is shown in Figures VI.1 and VI.2. Like the 85-pin reactor, the 19-pin core is in a hexagonal array that is encased by a 12-sided steel baffle. Nineteen homogenous fuel pins contain UO_2 enriched to 93% ^{235}U, SS-316 clad, and Gd_2O_3 poison. The fractions of each material are calculated from Marcille et al[4]. The density of the fuel was artificially increased in the MCNP input file to achieve a k_{eff} of approximately 1 with a 90 degree rotation of the control drums.

TABLE III. Design parameters for the 19-pin concept

Parameter	Value
Number of fuel pins	19
Fuel length (cm)	38
Axial reflector length (cm)	2
End cap length (cm)	0.5
Fission gas plenum length (cm)	1
Pin OD (cm)	2.108
Pin pitch	2.372
Fuel pellet OD	1.994
Fuel clad thickness	0.051
Inner basket wall thickness (cm)	0.1
Downcomer thickness (cm)	0.42
Vessel thickness (cm)	0.25
Control drum OD (cm)	8.1
Maximum reflector thickness (cm)	7.7
Water shield OD (cm)	21.46
Inner basket height (cm)	46.5
Vessel height (cm)	52.5
Reflector height (cm)	52.5

Outside of this inner vessel lies a downcomer region, and outside of the downcomer is the 0.25 cm SS-316 pressure vessel. The reactor uses six scaled-down external control drums encased in a cylindrical radial water shield, as depicted in the cross section view in Figure VI.2. The thin B_4C elements of the drums are shown in a "full in" (180 degrees) orientation in this figure, which would be the launch configuration if this were an actual reactor. The remainder of the drum elements and the interstitial radial reflector are composed of beryllium. The reactor utilizes a borated-water shield contained in a SS vessel.

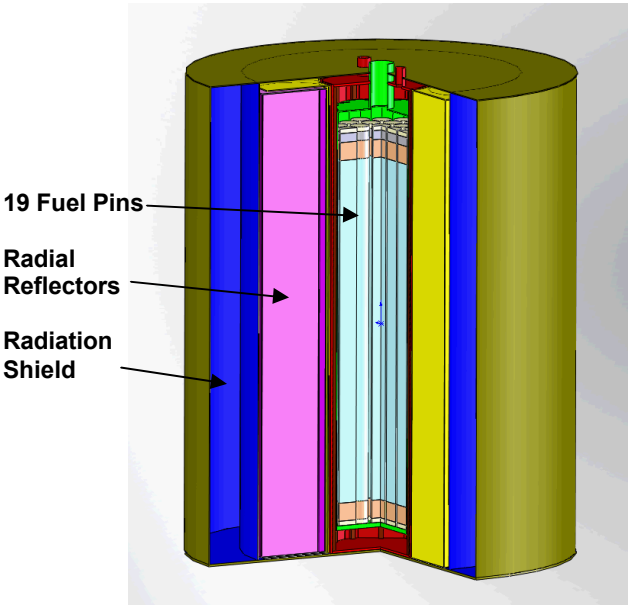

Figure VI.1: 19-pin reactor configuration

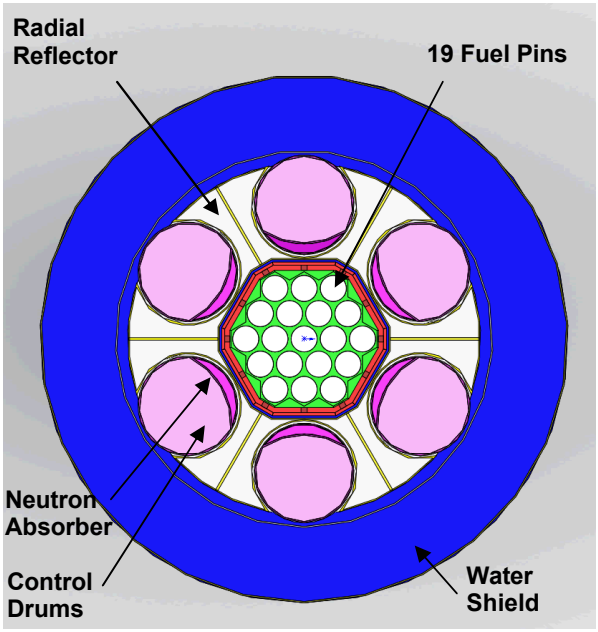

Figure VI.2: Top view of 19-pin reactor cross section

An MCNP input file was created by hand for the geometry described above. The k_{eff} with the control drums at 180 degree, full in, was 0.94119 with a standard deviation of 0.00092. The result with the control drums at 0 degrees, full out, was a k_{eff} of 1.02440 with a standard deviation of 0.00110. (See Table IV).

To compare these standard MCNP results with results obtained using DAG-MCNP5, the geometry (with control drums full in) was modeled in SolidWorks 2009 and then

imported into Cubit 10.2. Overlapping and duplicate surfaces were removed and a region of zero importance which bounded the problem was created. Material properties were also assigned within Cubit. The geometry was then exported as an ACIS geometry file and run with DAG-MCNP5. The results were a k_{eff} of 0.94095 with a standard deviation of 0.00092.

Inspection of the FEA results for the 19-pin reactor 40-m/s impact (Figure V.5) suggests that the fuel pins will be deformed in such a way that they will come into contact with neighboring pins in the lower region of the fuel. As a comparison for future DAG-MCNP5 runs with the 19-pin deformed geometry, an MCNP file with an approximated post impact geometry was created. The fuel was deformed such that the pins were just touching one another for the bottom 50% of the fuel. The upper portion of the fuel remained undeformed. The fuel length was shortened to conserve fuel volume. The reflector and control drums region was also shortened and subsequently widened to conserve volume. For a comparison run, the water shield was also shortened. (See Figure VI.3 and Figure VI.4)

This post-impact approximated geometry was run in various configurations with multiple surrounding materials. A base comparison was done with control drums full in and the water shield still intact. The reflectors, control drums, and water shield were then removed and this vessel only geometry was run with pure water, wet sand, and liquid hydrogen as surrounding materials. The results are shown in Table IV. The results for the undeformed geometry were added to the table also, for comparison purposes.

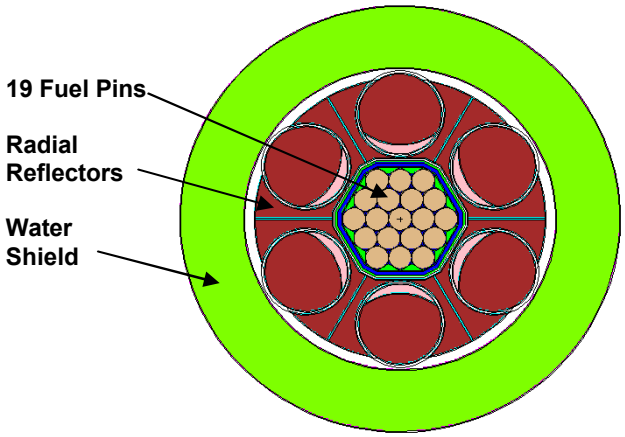

Figure VI.3 Lower portion fuel geometry in 19-pin post-impact approximated geometry

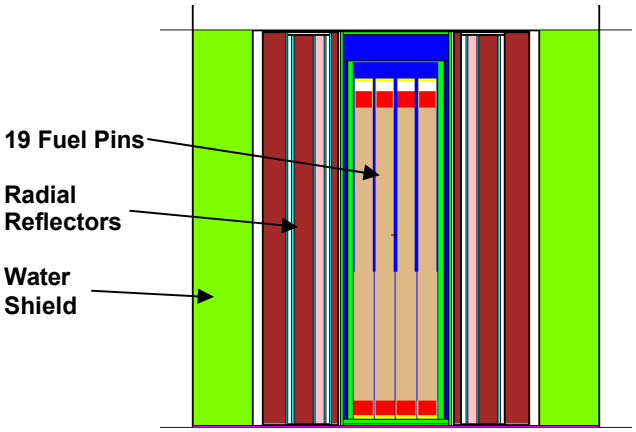

Figure VI.4. Front cross-sectional view of 19-pin post-impact approximated geometry

Table IV. MCNP Results for 19-pin Reactor Model

Status	Geometry (CD* position)	Surrounding Material	Keff (std dev)
Pre-Impact	Water Shield (0)	Void	1.02440 (0.00110)
Pre-Impact	Water Shield (180)	Void	0.94119 (0.00092)
Post-Impact	Water Shield (180)	Void	1.02292 (0.00098)
Post-Impact	Pressure Vessel (NA)	Water	0.98582 (0.00107)
Post-Impact	Pressure Vessel (NA)	Wet Sand	1.03066 (0.00103)
Post-Impact	Pressure Vessel (NA)	Liquid H_2	0.93010 (0.00101)

* Control Drum, 0 degrees is full out, 180 is full in

The previous results are interesting, but were obtained with a non-physical design. The density of the fuel in the 19-pin reactor was artificially increased to make the k_{eff} near critical. To determine if the behavior seen in the 19-pin design is still valid, the 85-pin reactor design[4] was run with all the same geometries. Figure VI.5 shows a cross section of the core prior to the impact modifications. Similar to the 19-pin case, the lower 50% of the 85-pin model was modified so that the pins were in contact with each other. The results can be seen in Table V. The total reactivity change for the 85-pin reactor (about 0.1) is about the same as for the 19-pin reactor. But the 85-pin reactor remains subcritical by a substantial margin after impact because it has a lower initial reactivity in shutdown mode.

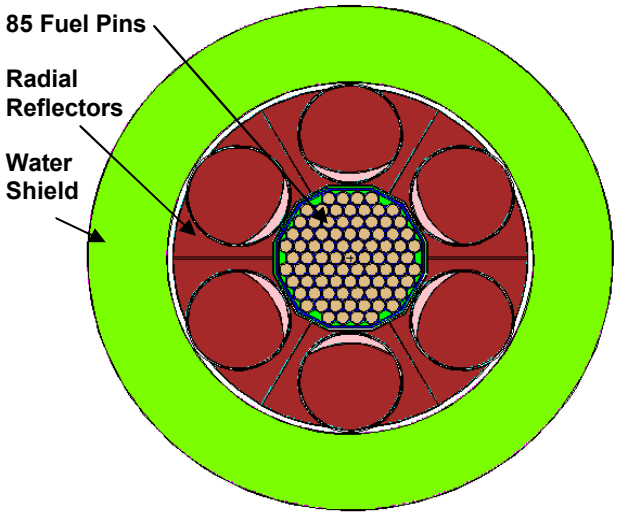

Figure VI.5. Top cross-sectional view of 85-pin, pre-impact geometry

Table V. MCNP Results for 85-pin Reactor Model

Status	Geometry (CD* position)	Surrounding Material	Keff (std dev)
Pre-Impact	Water Shield (0)	Void	1.02072 (0.00096)
Pre-Impact	Water Shield (180)	Void	0.86142 (0.00101)
Post-Impact	Water Shield (180)	Void	0.90915 (0.00076)
Post-Impact	Pressure Vessel (NA)	Water	0.88644 (0.00105)
Post-Impact	Pressure Vessel (NA)	Wet Sand	0.95541 (0.00098)
Post-Impact	Pressure Vessel (NA)	Liquid H_2	0.81910 (0.00092)

* Control Drum, 0 degrees is full out, 180 is full in

VII. CONCLUSIONS

A method for determining the change in reactivity in a space reactor following impact during a launch accident has been described. An existing continuum mechanics code (Pronto3D) has modeled the impact of a 19-pin reactor concept in 24 hours using 300 processors. More realistic configurations with more fuel pins would take more time and processors, but this looks feasible. Transferring the deformed geometry to a criticality code (MCNP) is challenging, but a transfer code (DAGMC) has made a successful transfer of a very simple test case after some modification. This bodes well that transfer and reactivity modeling of a prototypic space reactor might be feasible with continued development.

ACKNOWLEDGMENTS

The authors thank David Harding for his assistance in the preliminary determination of UO_2 mechanical properties. The work for this paper was supported the Laboratory Directed Research and Development program at Sandia National Laboratories. Sandia is a multiprogram laboratory operated by Sandia Corporation, a Lockheed Martin Company, for the United States Department of Energy under Contract DE-AC04-94AL85000.

REFERENCES

1. R. F. WILSON, H. M. Dieckamp and D. J. Cockeram,, "SNAP 10A Design, Development, and Flight Test," AIAA Second Annual Meeting, San Francisco, CA, July 26-29, 1965, AIAA Paper No. 65-467 (1965).

2. V, C. TRUSCELLO and L. L. Rutger, "The SP-100 Power System," *Proceedings of the 9th Symposium on Space Nuclear Power Systems*, Albuquerque, NM, January 15, 1992, CONF 920104, AIP CP246, Issue 1 (1992).

3. J. ASHCROFT and C. Eshelman, "Summary of NR Program Prometheus Efforts," *Proceedings of the Space Technology and Applications International Forum—STAIF2007*, Albuquerque, NM, February 11, 2007, AIP Conf. Proc., CP880, pp 497-521 (2007).

4. T. F. MARCILLE, D. D. Dixon, G. A. Fischer, S. P. Doherty, D. I. Poston and R. J. Kapernick, "Design of a Low Power, Fast-Spectrum, Liquid-Metal Cooled Surface Reactor System," *Proceedings of the Space Technology and Applications International Forum—STAIF2006*, Albuquerque, NM, February 12-16, 2006, AIP Conf. Proc., CP813, pp 319-326 (2006).

5. D. I. POSTON, R. J. Kapernick, D. D. Dixon, B. W. Amiri, T. F. Marcille, "Reference Reactor Module for the Affordable Fission Surface Power System," *Proceedings of the Space Technology and Applications International Forum—STAIF2008*, Albuquerque, NM, February 10-14, 2008, AIP Conf. Proc., CP969, pp 277-284 (2008)..

6. J. O. ELLIOTT, R. J. Lipinski and D. I. Poston, "Mission Concept for a Nuclear Reactor-Powered Mars Cryobot Lander," *Proceedings of the Space Technology and Applications International Forum—STAIF2003*, Albuquerque, NM, February 2-5, 2003, AIP Conf. Proc., CP654, pp 353-360 (2003).

7. R. J. LIPINSKI, S. A. Wright, M. P. Sherman, R. X. Lenard, R. A. Talandis, D. I. Poston, R. Kapernick, R. Guffee, R. Reid, J. Elson and J. Lee, "Small Fission

Power Systems for Mars," *Proceedings of the Space Technology and Applications International Forum—STAIF2002*, Albuquerque, NM, February 3-6, 2002, AIP Conf. Proc., CP608, pp 1043-1053 (2002).

8. M. KLEIN, "Nuclear Thermal Rocket – An Established Space Propulsion Technology," *Proceedings of the Space Technology and Applications International Forum—STAIF2004*, Albuquerque, NM, February 8-11, 2004, AIP Conf. Proc., CP699, pp 413-419 (2004).

9. J. A. DEWAR, *To the End of the Solar System, The Story of the Nuclear Rocket*, Second Edition, Apogee Books, Collector's Guide Publishing, Inc., Burlington, Ontario, Canada, pp. 110, 179-184 (2007).

10. E. J. PARMA, R. M. Bass, G. S. Hoovler, E. C. Selcow and R. J. Cerbone, "A Critical Assembly Designed to Measure Neutronic Benchmarks in Support of the Space Nuclear Thermal Propulsion Program," *Proceedings of the Tenth Symposium on Space Nuclear Power Systems,* Albuquerque, NM, January 16. 1993, AIP Conf. Proc, CONF 930103, pp. 785-793 (1993).

11. J. C. KING and M. S. El-Genk, "A Methodology for the Neutronics Design of Space Nuclear Reactors," *Proceedings of the Space Technology and Applications International Forum—STAIF2004*, Albuquerque, NM, February 8-11, 2004, AIP Conf. Proc., CP699, pp 319-329 (2004)

12. J. C. KING and M. S. El-Genk, "Spectral Shift Absorbers for Fast Spectrum Space Nuclear Reactors," *Proceedings of the Space Technology and Applications International Forum—STAIF2005*, Albuquerque, NM, February 10-14, 2005, AIP Conf. Proc., CP746, pp 285-294 (2005)

13. Y. WU and X. George Xe, "The Need for Further Development of CAD/MCNP Interface Codes," *Computational Medical Physics Radiation Modeling,* pp. 392-394 (2007)

14. M. SAWAN, P. Wilson, T. Tautges, L. El-Guebaly, D. Henderson, et al., "Innovative Three-Dimensional Neutronics Analyses Directly Coupled with CAD Models of Geometrically Complex Fusion Systems," *Proceedings of the 13th International Conference on Emerging Nuclear Energy Systems*, Istanbul, Turkey, June 3-8, 2007.

15. T. J. TAUTGES, Ray Meyers, Kerl Merkley, Clint Stimpson, and Corey Ernst, *MOAB: A mesh-oriented database*, Technical Report SAND2004-1592, Sandia National Laboratories, Albuquerque, NM (2004).

16. SANDIA NATIONAL LABORATORIES, Cubit Geometry and Mesh Generation Toolkit, 19 February 2009, http://cubit.sandia.gov (2009).

17. S. W. ATTAWAY, F.J. Mello, M.W. Heinstein, J.W. Swegle, J.A. Ratner, R.I. Zadoks, "Pronto 3D Users Instructions: Transient Dynamic Code for Nonlinear Structural Analysis, SAND98-1361, Sandia National Laboratories, Albuquerque NM (1998).

18. L.A. SCHOOF, V.R. Yarberry, *EXODUS II: A finite Element Data Model*, Technical Report SAND92-2137, Sandia National Laboratories, Albuquerque NM, (1994).

19. BATTELLE'S COLUMBUS DIVISION, *Structural Alloys Handbook*, Vol. 3, Columbus OH (1986).

20. BATTELLE'S COLUMBUS DIVISION, *Structural Alloys Handbook*, Vol. 2, Columbus OH (1986).